Desalination and Water Treatment
www.deswater.com
doi: 10.5004/dwt.2023.29747

303 (2023) 59–69
August

Simultaneous removal of nitrogen and phosphorus from urban sewage by synthetic zeolites adsorption: performance, characterization, and mechanism

Rui Zhao[a], Guangzhi Wang[a,*], Hongfang Chen[a], Simin Zhou[a], Xiyu Sun[a], Dongdong Wang[a], Likun Huang[b,*], Zhe Li[b]

[a]*School of Environment, Harbin Institute of Technology, 73 Huanghe Road, Harbin 150090, China, emails: hitwgz@126.com (G. Wang), ruizhao2019@yeah.net (R. Zhao), cxj99521@qq.com (H. Chen), 1148295955@qq.com (S. Zhou), wo13884979274@163.com (X. Sun), 2447003974@qq.com (D. Wang)*
[b]*School of Food Engineering, Harbin University of Commerce, Harbin 150076, China, emails: hlk1980@163.com (L. Huang), Alisazhe@163.com (Z. Li)*

Received 13 August 2022; Accepted 3 July 2023

ABSTRACT

It is difficult for the urban sewage effluent after secondary treatment to satisfy the standard of urban sewage reuse and recycle, which has a low concentration of nitrogen and phosphorus greatly leading to serious water eutrophication and environmental pollution. This study novelty proposed a kind of synthetic zeolites for effectively removing nitrogen and phosphorus in-depth from urban sewage, the characterization and adsorption mechanism were studied. Results showed an appropriate synthetic zeolites addition (3.0–6.0 g·L^{-1}) could result in a high removal efficiency (TN: 60.32%, NH_4^+–N: 77.5%, PO_4^{3-}–P: 99.9%). Simultaneously, the X-ray diffraction, scanning electron microscopy, and Brunauer–Emmett–Teller analysis showed that the synthetic zeolites were mesoporous materials with large specific surface area and uneven pore-size distribution. Further, the adsorption isotherms followed the Freundlich model (R^2 = 0.99), thereby confirming a heterogeneous adsorption of nitrogen and phosphorus by the synthetic zeolites. The PO_4^{3-}–P adsorption was complexation effect between PO_4^{3-} and aluminum complexes in the synthetic zeolites, and NH_4^+–N adsorption by the synthetic zeolites was ion exchange between NH_4^+ and Na^+. Finally, the equilibrium adsorption capacity of recycled synthetic zeolites proved a good reusability by showing an equivalence to that of initial synthetic zeolites. This study provided a potential strategy for cost-effective use of zeolites on urban sewage treatment.

Keywords: Urban sewage; Nitrogen; Phosphorus; Synthetic zeolites; Kaolin

1. Introduction

The reuse and recycle of urban sewage are the key solution to insufficient water supplies, which also reduces effluent discharge and offers a reliable alternative water supply for freeing up limiting drinking water resources [1]. At present, the reuse and recycle treatment of urban sewage are primarily applied to sewage irrigation, municipal greening, and groundwater recharge [2,3]. However, due to a high and stable nitrogen solubility which originated from agricultural fertilizers in recycled sewage, it is easy to transport with recycled sewage and become the most common environmental risk of recycled sewage pollution all over the world [3,4]. Simultaneously, there are still phosphorus that cannot be removed in sewage after secondary treatment, of which excessive discharge with nitrogen together into aquatic environments can cause one of the most severe water perturbations – eutrophication phenomenon [5,6]. Therefore,

* Corresponding authors.

the nitrogen and phosphorus pollution in urban sewage needs in-depth treatment to satisfy the standard of urban sewage reuse and recycle.

Diverse processes have been widely used to simultaneously remove nitrogen and phosphorus from urban sewage. Biological treatments such as anaerobic/anoxic/aerobic processes are widely applied as their low-cost requirements [7–9]. However, these processes have common disadvantages concerning the simultaneous nitrogen and phosphorus removal, and it is sensitive for bacteria to adapt changeable pH and temperature or extreme environmental conditions. Notably, these processes have a better removal performance only applying to high concentration nitrogen and phosphorus, which is also known to be time-consuming. Besides, chemical treatments for nitrogen and phosphorus removal such as chemical sedimentation are highly depend on pH and temperature and have a high energy and agent cost [11]. Physico-chemical treatments, for example, adsorption technology, which is considered by Environmental Protection Agency of United States (EPA) to be the most effective method for urban sewage treatment, especially the nitrogen removal [12–14]. Therefore, it is a feasible strategy of adsorption method for nitrogen and phosphorus removal. Currently, the main challenge of adsorption method is to find novel adsorption materials with low cost, stable removal performance and a high recovery rate.

Zeolites, a class of hydrated aluminosilicate compounds, is formed by AlO_4 and SiO_4 connected by sharing an oxygen atom with a three-dimensional framework structure [15]. It is a kind of commonly used adsorption materials, which has electro-negativity, rich pore structure and huge specific surface area to provide rich adsorption sites for material adsorption [16,17]. And it is easy for zeolites to regenerate and recycle without losing their adsorption characteristics significantly [14]. In addition, for treating low molecular weight pollutants, the mesoporous structure of zeolites provides more selectivity and they are stable at wide intervals of pH and temperature [15,18]. These superior properties of zeolite nanoparticles make it advantageous for working out the stability problem, incomplete conversion, and generation of less toxic by-products in system [19]. Therefore, they are widely used in wastewater treatment and even more extensive fields as an excellent property of adsorption, catalysis, and ion exchange [16]. Natural zeolites have an effective adsorption effect on ammonia nitrogen (NH_4^+–N). Wang et al. [20] used zeolite powder as absorbent to quickly reach absorption equilibrium of NH_4^+–N after 10 min. Lin et al. [21] studied the adsorption performance improvement and adsorption mechanism of NH_4^+–N by NaCl-modified zeolites, which can change surface morphology by increasing the sodium contents for improving the mass transfer rate on the membrane. And Guo et al. [22] also utilized zeolites of the biochar-zeolites to selectively remove the NH_4^+–N in the biogas slurry including NH_4^+–N, PO_4^{3-}–P, and arsenic (As^{3+}). However, there are still some deficiencies for nitrogen and phosphorus removal. Although natural zeolites can effectively adsorb cationic pollutants such as NH_4^+–N in urban sewage as the structural electro-negativity, they have a poor removal effect on anionic pollutants such as nitrate and phosphate [23]. For example, Lee et al. [24] proposed to use mussel and oyster shell wastes to remove phosphorus from eutrophic lakes, but the nitrogen would not be adsorbed simultaneously with the process of phosphorus removal. Therefore, it is necessary to artificially synthesize zeolites with effective removal performance on both nitrogen and phosphorus.

In this study, the adsorption technology by the synthetic zeolites was proposed to remove nitrogen and phosphorus simultaneously. Thus, the main objectives of this study were (1) to synthesize a kind of novel zeolite with a stable structure and a high adsorption capacity, (2) to remove NH_4^+–N and PO_4^{3-}–P with the synthetic zeolites for improving nitrogen and phosphorus removal performance, (3) to further explore the mechanism on nitrogen and phosphorus removal with the synthetic zeolites by adsorption kinetics fitting and adsorption isothermal fitting. The main aims of this study were to propose a kind of novel synthetic zeolites as the adsorption material to remove nitrogen and phosphorus simultaneously for the reusing and recycling the urban sewage.

2. Materials and methods

2.1. Preparation and characterization of the synthetic zeolites

As shown in Fig. 1, the zeolites were synthesized by using kaolin as raw materials, which the kaolin ($Al_2O_3{\cdot}2SiO_2{\cdot}2H_2O$) was activated in muffle furnace at 650°C (2 h) for obtaining metakaolin, and the heating rate was 30°C/min. The NaOH (100 mL) and metakaolin was added to conical flask (250 mL), which was put on a heating magnetic stirrer at a rotational speed of 400 rpm. The molar ratio between Na_2O

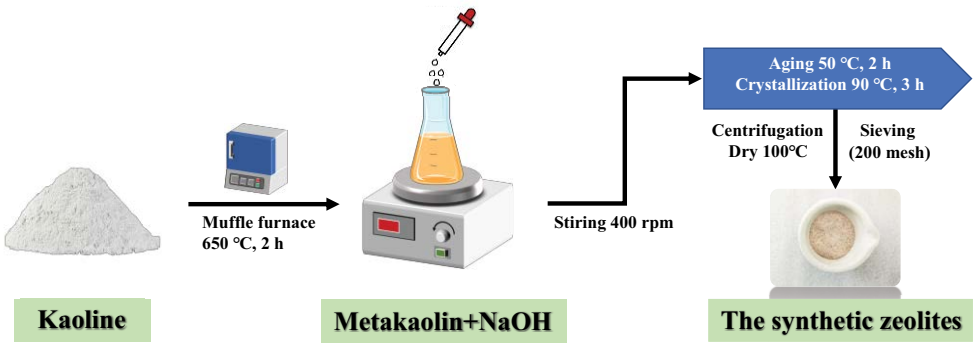

Fig. 1. Preparation of the synthetic zeolites.

and SiO_2 was marked as $n(Na_2O)/n(SiO_2)$, and the molar ratio between H_2O and Na_2O was marked as $n(H_2O)/n(Na_2O)$, which were 2:1 and 40:1, respectively. The aging and crystallization reaction stage has adjusted at 50°C (2 h) and 90°C (3 h), respectively. After the reaction, they were centrifuged for separation completely (the pH of supernatants approached to neutral). The products were dried at 100°C and pounded after cleaning. The synthetic zeolites were obtained by passing through 200 mesh sieve, and then they were put in a desiccator for standing by.

Simultaneously, the Brunauer–Emmett–Teller (BET, Quadrasorb SI-MP, Quantachrome, USA) method was used to measure the specific surface area of zeolites [25]. The surface morphology of zeolites was observed by scanning electron microscopy (SEM, ZEISS Sigma 500, UK) with an extraction voltage of 3.86 kV [26]. The components and structure of zeolites were obtained by X-ray diffractometer (XRD, D8 Advance, Bruker, UK) with a scan range from 3° to 70° 2θ at a scan speed of 1°/min [25]. And the voltage and current were set at a 40 mV and 40 mA.

2.2. Composition of synthetic wastewater

For investigating the adsorption performance of nitrogen and phosphorus by synthetic zeolites, the synthetic wastewater was composed of total nitrogen (TN) (20 mg·L^{-1}) and PO_4^{3-}–P (2 mg·L^{-1}), which included NH_4^+–N (10 mg·L^{-1}).

2.3. Removal performance and mechanism of nitrogen and phosphorus adsorption by the synthetic zeolites

2.3.1. Removal performance of nitrogen and phosphorus adsorption by the synthetic zeolites

The synthetic zeolites (0.2, 0.6, 1.0, 1.4, 2.0, 3.0, 4.0, 6.0, 10.0, 14.0, and 20.0 g·L^{-1}) was respectively put into conical flasks with synthetic wastewater (50 mL, pH 5), and oscillated at 150 rpm, 20°C ± 0.5°C, and the samples were measured through 0.45 μm filtration membrane periodically. All experiments were performed in triplicate to reduce experimental errors. The concentration of NH_4^+–N, TN, PO_4^{3-}–P was measured using standard methods [27] by ultraviolet spectrophotometer (Purkinje General T6, Beijing, China).

2.3.2. Fitting of the Langmuir and Freundlich adsorption model

A series of different initial concentration PO_4^{3-}–P solution (2, 5, 10, 20, and 50 mg·L^{-1}; 50 mL) and initial concentration NH_4^+–N solution (5, 10, 20, 50, and 100 mg·L^{-1}; 50 mL) was adjusted to pH 5, and then mixed with the synthetic zeolites (6.0 g·L^{-1}) in a water bath thermostatic oscillator (HZQ-, HDL, Beijing, China) at 150 rpm, 20°C ± 0.5°C for 2 h. Eventually, the samples were measured through 0.45 μm filtration membrane.

The Langmuir isothermal adsorption model was generally utilized to describe the monolayer adsorption on the surface of adsorbents. The Langmuir isothermal adsorption model was as follows [28]:

$$\frac{C_e}{Q_e} = \frac{1}{Q_{\max}} C_e + \frac{1}{Q_{\max} k_L} \tag{1}$$

The Freundlich isothermal adsorption model was used to describe the process of heterogeneous adsorption on the surface of adsorbents. The equation was as follows [29]:

$$\ln Q_e = \ln k_f + \frac{1}{n} \ln C_e \tag{2}$$

where k_L – Langmuir constant (L·mg^{-1}); k_f – Freundlich constant (mg$^{1-1/n}$·(L$^{1/n}$·g)); Q_e – adsorption capacity at equilibrium (mg·g^{-1}); $Q_{\max}$ – maximum adsorption capacity (mg·g^{-1}); C_e – solution concentration at equilibrium (mg·L^{-1}); $1/n$ – heterogeneous factor.

2.3.3. Fitting of the pseudo-first-order and pseudo-second-order adsorption kinetics

A series of different initial concentration PO_4^{3-}–P solution (2, 5 mg·L^{-1}; 50 mL) and initial concentration NH_4^+–N solution (5, 10 mg·L^{-1}; 50 mL) were adjusted to pH 5, and then oscillated mixing with the synthetic zeolites (6.0 g·L^{-1}) at 150 rpm, 20°C ± 0.5°C (2 h). Finally, the samples were measured through 0.45 μm filtration membrane.

The pseudo-first-order kinetics equation was as follows:

$$\ln\left(Q_e - Q_t\right) = \ln Q_e - k_1 t \tag{3}$$

And the pseudo-second-order kinetics equation was as follows [30]:

$$\frac{t}{Q_t} = \frac{1}{k_2 Q_e} + \frac{t}{Q_e} \tag{4}$$

where k_1 – pseudo-first-order adsorption rate constant (1 min^{-1}); k_2 – rate constant of pseudo-second-order kinetics (g(mg·min^{-1})); t – time (min); Q_e – adsorption capacity at equilibrium (mg·g^{-1}); Q_t – the capacity of the adsorbents at specific time (mg·g^{-1}).

2.4. Recycle experiment of the synthetic zeolites for nitrogen and phosphorus adsorption

The synthetic zeolites after reaction were centrifuged until the supernatants near neutral, and were centrifuged with percutaneous ethanol for twice. And finally percutaneous ethanol was removed by DI water. After cleaning, the zeolites were put into a drying oven (PH-030A, Yi Heng, Shanghai, China) at 110°C for 2 h. The dried zeolites (1.0 g) were added into NaOH solution (0.2 mol·L^{-1}), centrifuged until neutral for 10 h, and dried eventually. The synthetic zeolites (6.0 g·L^{-1}) were added into the solution of PO_4^{3-}–P (2 mg·L^{-1}) and NH_4^+–N (5 mg·L^{-1}) after cleaning. The samples were measured through 0.45 μm filtration membrane at specific times (1, 3, 5, 10, 15, 30, 45, 60, 90, 120, and 180 min, respectively).

3. Results and discussions

3.1. Effect of synthetic zeolites dosage on nitrogen and phosphorus adsorption performance

The thermogravimetric analysis of the synthetic zeolites was carried out with a heating rate of 5°C/min below

900°C, which is shown in Fig. 2. The structure of products tended to be stable up to 650°C due to a complete release of water, and the suitable activated temperature at about 600°C–800°C, considered of energy consumption, the activated temperature was lastly set at 650°C.

The nitrogen and phosphorus adsorption performance by the synthetic zeolites is shown in Fig. 3a. The removal efficiency of TN was increased with zeolites dosage of 0.2–4.0 g·L^{-1} and remained above 60% along with zeolites dosage of 6.0–20.0 g·L^{-1}. Simultaneously, along with zeolites dosage of 0.2–6.0 g·L^{-1}, the removal efficiency of NH_4^+–N obviously increased and remained above 80% with zeolites dosage of 10.0–20.0 g·L^{-1}. Within the scope of zeolites dosage, there was no desorption process. An appropriate zeolites dosage was 3.0–20.0 g·L^{-1}, which can ensure the NH_4^+–N removal above 68%. In addition, the removal efficiency of PO_4^{3-}–P was rapidly increased with zeolites dosage of 0.2–1.4 g·L^{-1}, and up to zeolites dosage of 2.0–4.0 g·L^{-1}, the adsorption efficiency remained above 99%. However, the PO_4^{3-}–P removal was slowed down along with zeolites dosage increase of 6.0–20.0 g·L^{-1}. With the increasing of the dosage of zeolites, the provided adsorption sites also increased correspondingly, the PO_4^{3-}–P removal efficiency was reduced because the adsorption capacity of the single adsorption site was limited by applied force between multiple adsorption sites and the PO_4^{3-}–P. Therefore, a suitable dosage of zeolites was 3.0–6.0 g·L^{-1}, which can keep the PO_4^{3-}–P removal efficiency above 93%. In Fig. 3b and c, the removal efficiencies of phosphorus show a rapid increase with the increase of the dosage of synthetic zeolites (2.0–6.0 g·L^{-1}). The highest removal efficiencies reached 99.123% at 6.0 g·L^{-1} synthetic zeolites addition, the max phosphorus adsorption capacity reached 2.035 mg·g^{-1} with 0.6 g·L^{-1} synthetic zeolites. And the removal efficiencies of NH_4^+–N showed a rapid increase with the increase of the dosage of synthetic zeolites (0.2–1.4 g·L^{-1}). The highest removal efficiencies reached 69.382% at 1.6 g·L^{-1} synthetic zeolites addition, the max NH_4^+–N adsorption capacity reached 20.595 mg·g^{-1} with 0.2 g·L^{-1}

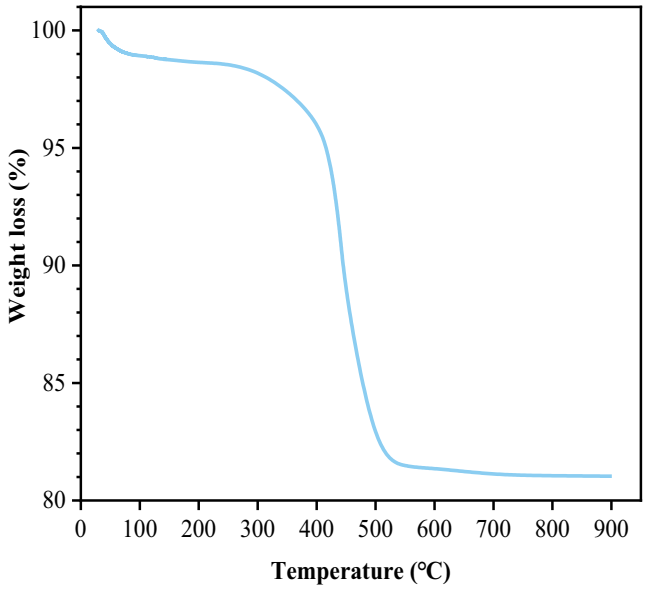

Fig. 2. Thermogravimetric analysis of the synthetic zeolites.

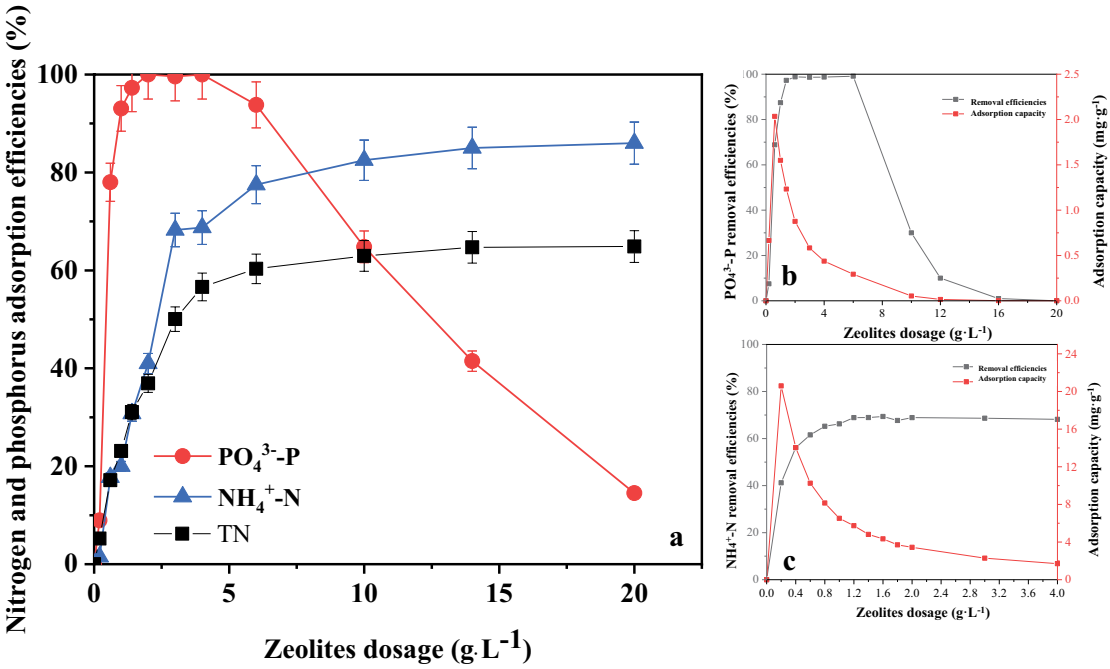

Fig. 3. Nitrogen and phosphorus adsorption performance by zeolites, the zeolites dosage: 0.2, 0.6, 1.0, 1.4, 2.0, 3.0, 4.0, 6.0, 10.0, 14.0, and 20.0 g·L^{-1} (a), individual phosphorus adsorption performance by various dosages of synthetic zeolites (the zeolites dosage: 0.2, 0.6, 1.0, 1.4, 2.0, 3.0, 4.0, 6.0, 10.0, 14.0, and 20.0 g·L^{-1}) (b), individual NH_4^+–N adsorption performance by various dosage of synthetic zeolites (NH_4^+–N, 10 mg, the zeolites dosage: 0.2, 0.6, 0.8, 1.0, 1.2, 1.4, 1.6, 1.8, 2.0, 3.0, and 4.0 g·L^{-1}) (every point with an error bar was symbolized the mean ± standard deviation, respectively).

synthetic zeolites. Compared with individual NH_4^+–N adsorption, the removal efficiencies were increased by about 8%, which indicated that the co-occurrence of nitrogen and phosphorus was more conducive to the NH_4^+–N adsorption. And it had little effect for phosphorus adsorption between the condition of co-occurrence of nitrogen and phosphorus and individual phosphorus.

The previous studies focus on the zeolites applied as ion exchangers and adsorbents in numerous areas of agriculture and environmental protection, which ascribes to their particular characteristics. The main focus of attention in agriculture is currently on natural zeolites which can be a useful soil conditioner and an additive to fertilizer [31]. And the natural zeolites were utilized to adsorb PO_4^{3-}–P with a low adsorption capacity [32], compared to this, the synthetic zeolites were mainly used for environmental remediation [33–35], which has a huge advantage on achieving a high phosphorus removal efficiency. Besides, the previous studies mainly focus on zeolites modification, which the approach was complex and time-consuming. For example, Wan et al. [31] produced a kind of zeolites, which the NH_4^+–N and PO_4^{3-}–P decreased from the initial 756.9 mg·L^{-1} and 106.5 mg·L^{-1} to 201.1 mg·L^{-1} and 11.9 mg·L^{-1}, respectively, with the recovery rates of 70.5% and 84.3% after 5 h. Zhang et al. [36] prepared a kind of La-modified zeolites for NH_4^+–N, PO_4^{3-}–P adsorption (50 and 60 mg·L^{-1}). These studies had high removal efficiencies only for high concentration of NH_4^+–N, PO_4^{3-}–P adsorption. Although the removal efficiencies were approximate with our study, the NH_4^+–N still kept high in effluent, the NH_4^+–N in effluent in this study was 2.25 mg·L^{-1}, and the addition dosage of zeolites was high (20 and 10 g·L^{-1}) compared with this study (3.0–6.0 g·L^{-1}). Thus, the synthetic zeolites in this study were more effective and economical.

It was suggested that the synthetic zeolites exerted a positive effect on nitrogen and phosphorus adsorption performance. And considering the effect of different zeolites dosage on the adsorption performance of TN, NH_4^+–N, PO_4^{3-}–P, the appropriate zeolites dosage was about 3.0–6.0 g·L^{-1}, in which the TN removal efficiency was 50.05%–60.32%, the NH_4^+–N removal efficiency was 68.25%–77.5%, and the PO_4^{3-}–P removal efficiency was 93.8%–99.9%.

3.2. Characteristics of the synthetic zeolites on structure and surface topography

A kind of novel synthetic zeolites was produced in this study, which was obtained with kaolin as raw materials. And the synthetic zeolites were roasted on high temperature for activating kaolin and reducing organic impurities. The specific structure and surface topography of a material extremely affects the adsorption and ion exchange properties. Therefore, it was used to further discuss the adsorption performance and the adsorption mechanism of the synthetic zeolites. The XRD, SEM, and BET was measured for further characterizing the structure and surface topography of synthetic zeolites (Fig. 4). As shown in Fig. 4a and b, it was the standard XRD spectrogram of zeolite – A(Na) and the XRD spectrogram of the synthetic zeolites. The difference between peaks shape and diffraction peaks indicated the crystallinity and the phase diversity [26]. Further, the diffraction peaks of the synthetic zeolites almost correspond to the diffraction peaks of zeolite – A(Na) literally, which indicated that the synthetic zeolites were a kind of zeolite – A(Na) with

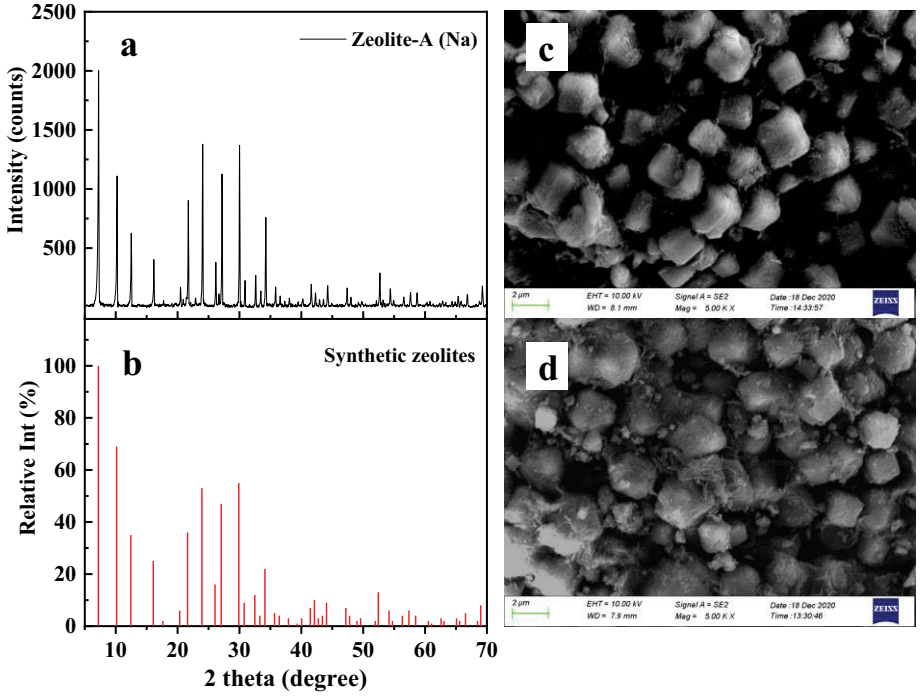

Fig. 4. X-ray diffraction spectrogram of standard zeolite – A(Na) (a), the synthetic zeolites (b), the scanning electron microscopy of the synthetic zeolites (c), the scanning electron microscopy of the synthetic zeolites after reaction.

an ideal purity. The SEM was utilized to reflect the surface characteristics, particle morphology, and various physical and chemical properties of the synthetic zeolites more clearly [36]. In Fig. 4c, the synthetic zeolites were regular hexahedron configuration with sharp edges and angles, which indicated that the crystallization effect was stable during the synthesis process. After the synthetic zeolites were contacted the water samples needed treatment, the edges and angles became relatively smooth, and there were more impurities on the surface of synthetic zeolites, which may be due to the presence of impurities in the water and the collision between the synthetic zeolites and reactor during the oscillating process, resulting in the damage of edges and angles of the synthetic zeolites. However, the synthetic zeolites still kept in the normal hexahedron configuration after the reaction, indicating that the structure was relatively stable (Fig. 4d).

The BET was utilized to further explain the surface area properties of the synthetic zeolites, and the pore-size distribution of zeolites was also an important factor to affect the adsorption performance [37]. The adsorption and desorption curves and pore-size distribution are shown in Fig. 5a and b. A small average pore size of the synthetic zeolites was 12.28 nm, the total pore size was 0.35 $cm^3 \cdot g^{-1}$, and the specific surface area of multi-point adsorption was 113.4 $m^2 \cdot g^{-1}$. It was previously reported that the larger surface area and smaller pore-size distribution of zeolites could provide more exposed adsorption sites for NH_4^+–N and PO_4^{3-}–P to be exchanged, and it was easier for NH_4^+–N and PO_4^{3-}–P to diffuse in the channels of the synthetic zeolites [38]. By various characterizing methods, the synthetic zeolites have the property of large specific surface area, uneven pore-size distribution, an ideal crystallization and purity. Therefore, it can be concluded that the synthetic zeolites were mesoporous materials with large specific surface area and uneven pore-size distribution, which indicated that it had abundant porous structure for better adsorption performance [39].

3.3. Adsorption mechanism of nitrogen and phosphorus by the synthetic zeolites

The Langmuir and Freundlich isothermal adsorption models were usually used to describe the adsorption mechanism of the synthetic zeolites on PO_4^{3-}–P and NH_4^+–N removal (Fig. 6 and Tables 1 and 2).

The phosphorus adsorption by zeolites can mainly use Al in synthetic zeolites to combine H^+ in water to form Al^{3+} (1–1), and then the Al^{3+} would be combined with PO_4^{3-} (1–2). On the other hand, the hydrolysis reaction of Al^{3+} could formed $Al(OH)^{2+}$ (1–3, 1–5), which would combine with PO_4^{3-} to form stable complex (1–4, 1–6). During this process, Al^{3+} did not separate from zeolites and still existed in the form of zeolites. The mechanism was that PO_4^{3-} and the aluminum complex in zeolites can combine together by ionic bond [32,40], and PO_4^{3-}–P could be adsorbed and removed by zeolites through complexation effect.

$$Z-Al+H^+ \rightarrow Z-Al^{3+} \quad \text{(I)}$$

$$Z-Al^{3+}+PO_4^{3-} \rightarrow Z-Al-PO_4 \quad \text{(II)}$$

$$Z-Al^{3+}+2H_2O \rightarrow Z-Al(OH)_2^+ + 2H^+ \quad \text{(III)}$$

$$Z-Al(OH)_2^+ + PO_4^{3-} \rightarrow \left[Z-Al(OH)_2-PO_4\right]^{2-} \quad \text{(IV)}$$

$$Z-Al^{3+}+H_2O \rightarrow Z-Al(OH)^{2+}+H^+ \quad \text{(V)}$$

$$Z-Al(OH)^{2+}+PO_4^{3-} \rightarrow \left[Z-Al(OH)-PO_4\right]^- \quad \text{(VI)}$$

As shown in Fig. 6a and b, for the phosphorus adsorption, the Freundlich isothermal adsorption model (R^2 = 0.99) fitted more closely than the Langmuir isothermal adsorption model (R^2 = 0.96), which was consistent with the previous research [41]. And the heterogeneous factor $1/N$ = 0.62 indicated that a high adsorption capacity during the process of the phosphorus adsorption by the synthetic zeolites. Further, the phosphorus was mainly removed by chemical adsorption by the synthetic zeolites, which confirmed that PO_4^{3-}–P and the aluminum complex in zeolites were bonded by ionic bonds, and phosphorus was adsorbed by zeolites through complexation effect.

Simultaneously, the nitrogen removal by zeolites mainly uses the exchange between NH_4^+ and cation in zeolites, and

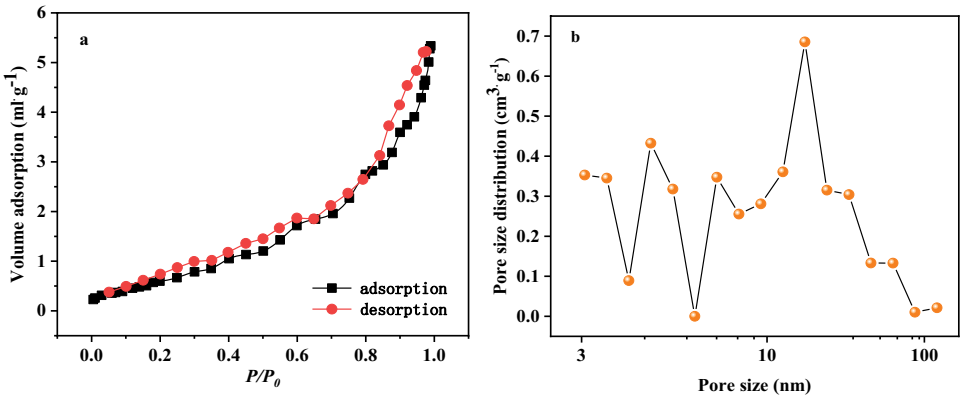

Fig. 5. Adsorption and desorption isotherms of N_2 by the synthetic zeolites (a), the pore-size distribution of the synthetic zeolites (b).

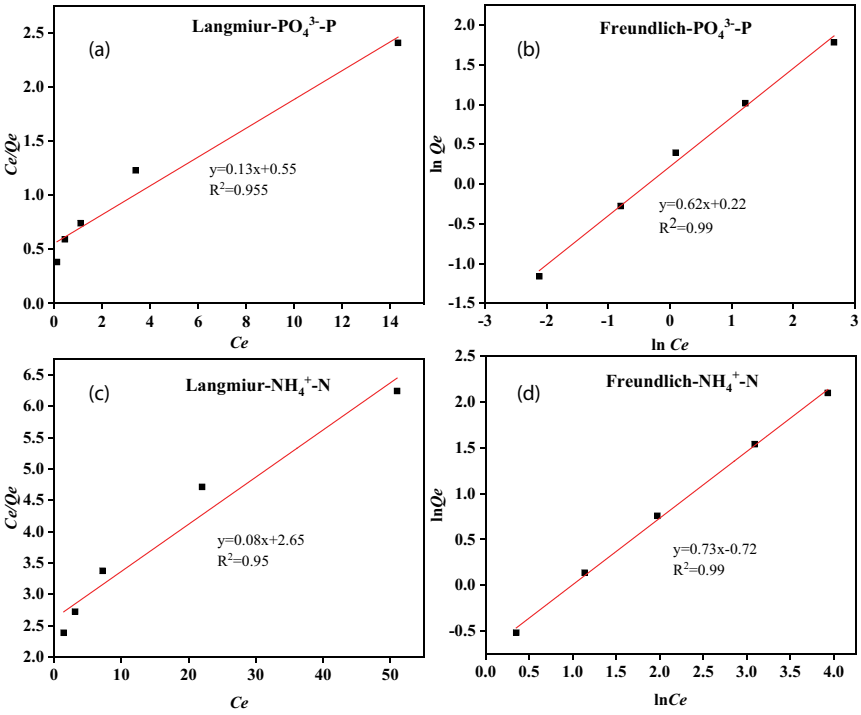

Fig. 6. Langmuir and Freundlich model fitting. The Langmuir model fitting of PO_4^{3-}–P and NH_4^+–N adsorption (a,c), the Freundlich model fitting of PO_4^{3-}–P and NH_4^+–N adsorption (b,d).

Table 1
Parameters of isothermal adsorption models for phosphorus adsorption by the synthetic zeolites

Langmuir			Freundlich		
Q_{max} (mg·g^{-1})	k_L (L·mg^{-1})	R^2	k_f (mg$^{1-1/n}$·(L$^{1/n}$·g))	1/n	R^2
7.5092	0.2401	0.95464	1.2465	0.6176	0.99312

Table 2
Parameters of isothermal adsorption models for nitrogen adsorption by the synthetic zeolites

Langmuir			Freundlich		
Q_{max} (mg·g^{-1})	k_L (L·mg^{-1})	R^2	k_f (mg$^{1-1/n}$·(L$^{1/n}$·g))	1/n	R^2
13.2943	0.0288	0.94518	0.4854	0.7228	0.99785

the NH_4^+ could replace the cations in the zeolites [32]. It was reported that the selecting order of common cations by zeolites was $K^+ > NH_4^+ > Na^+ > Ca^{2+} > Fe^{3+} > Al^{3+} > Mg^{2+}$ [42]. Therefore, the NH_4^+ could effectively replace a large amount of Na^+ in the zeolites, which was consistent with the previous research (1–7) [43].

$$Z-Na+NH_4^+ \rightarrow Z-NH_4^+ + Na^+ \quad \text{(VII)}$$

As shown in Fig. 6c and d, the Freundlich isothermal adsorption model (R^2 = 0.99) was more suitable for the NH_4^+–N adsorption by the synthetic zeolites than that of the Langmuir model (R^2 = 0.95), which was mainly chemically adsorbed by exchange between NH_4^+ and Na^+ in the synthetic zeolites [44]. The heterogeneous factor 1/N = 0.72, which indicated that the heterogeneous adsorption process of the NH_4^+–N by the synthetic zeolites has a high adsorption capacity [29]. A similar phenomenon and mechanism was also reported and supported on NH_4^+–N adsorption with natural zeolites, which the Ca^{2+} in the zeolites could be exchanged into the liquid for nitrogen removal [32].

Pseudo-first-order kinetics and pseudo-second-order kinetics model was utilized to fit the nitrogen and phosphorus adsorption by the synthetic zeolites. As shown in Fig. 7a, c and Table 3, the pseudo-second-order kinetics fitting (R^2 > 0.99) were greater than that of the pseudo-first-order kinetics. And the value of Q_e and k_2 were increased along with the increase of phosphorus concentration,

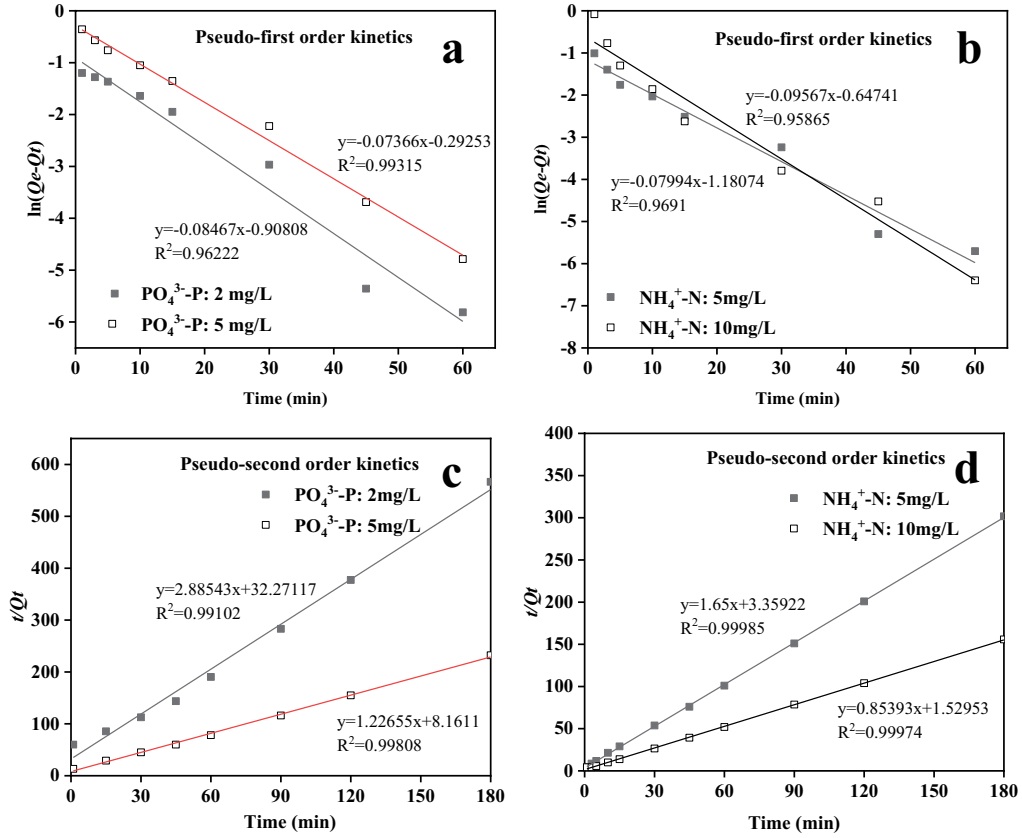

Fig. 7. Pseudo-first-order kinetics fitting for the PO_4^{3-}–P (a) and NH_4^+–N (b) adsorption by the synthetic zeolites, and pseudo-second-order kinetics fitting for the PO_4^{3-}–P (c) and NH_4^+–N (d) adsorption.

Table 3
Parameters of pseudo-first-order kinetics and pseudo-second-order kinetics for phosphorus adsorption by the synthetic zeolites

Initial PO_4^{3-}–P concentration ($mg \cdot L^{-1}$)	Pseudo-first-order kinetics			Pseudo-second-order kinetics		
	k_1 (min^{-1})	Q_e ($mg \cdot g^{-1}$)	R^2	k_2 ($g(mg \cdot min)^{-1}$)	Q_e ($mg \cdot g^{-1}$)	R^2
2	0.08467	0.318	0.96222	0.08930	0.347	0.99102
5	0.07366	0.775	0.99315	0.15035	0.815	0.99808

Table 4
Parameters of pseudo-first-order kinetics and pseudo-second-order kinetics for NH_4^+–N adsorption by the synthetic zeolites

Initial NH_4^+–N concentration ($mg \cdot L^{-1}$)	Pseudo-first-order kinetics			Pseudo-second-order kinetics		
	k_1 (min^{-1})	Q_e ($mg \cdot g^{-1}$)	R^2	k_2 ($g(mg \cdot min)^{-1}$)	Q_e ($mg \cdot g^{-1}$)	R^2
5	0.09567	0.5975	0.95865	0.4912	0.60607	0.99985
10	0.07994	1.1558	0.9691	0.5583	1.17106	0.99974

indicating that the driving force of adsorption between the synthetic zeolites and phosphorus became stronger [38].

As shown in Fig. 7b, d, and Table 4, the pseudo-second-order kinetics ($R^2 > 0.99$) fitted greater than that of the pseudo-first-order kinetics ($R^2 \geq 0.96$) for the NH_4^+–N adsorption. Similarly, with NH_4^+–N concentration increasing, the value of Q_e and k_2 were also increased, which indicated that the driving force of adsorption between the synthetic zeolites and NH_4^+–N became stronger.

As discussed above, the Freundlich isothermal adsorption model fitted more for the nitrogen and phosphorus adsorption by the synthetic zeolites, suggesting that the nitrogen and phosphorus could be removed effectively by chemical adsorption. And the pseudo-second-order kinetics

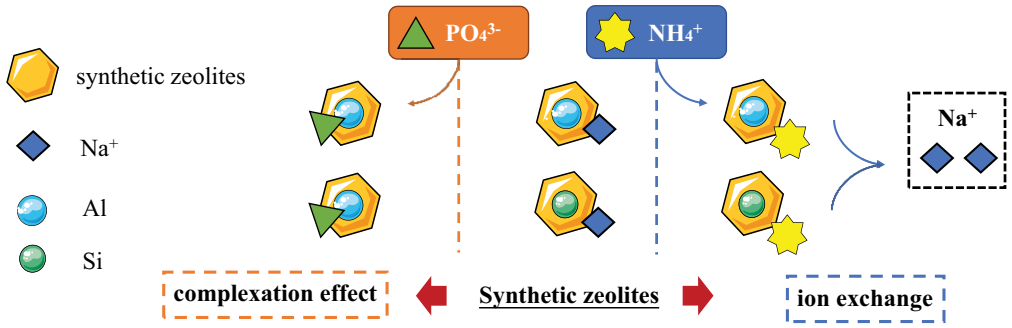

Fig. 8. Mechanism of the PO_4^{3-}–P and NH_4^+–N adsorption by synthetic zeolites.

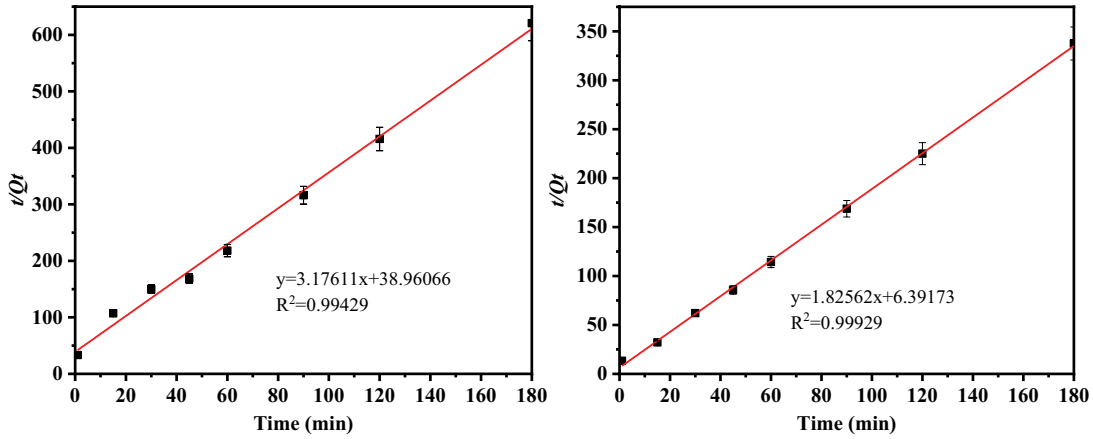

Fig. 9. Pseudo-second-order kinetics fitting on PO_4^{3-}–P (a) and NH_4^+–N (b) adsorption by the recycled synthetic zeolites (every point with an error bar were symbolized the mean ± standard deviation, respectively).

fitting was more suitable for describing these processes. As shown in Fig. 8, the mechanism of phosphorus was the ionic bond between PO_4^{3-}–P and the aluminum complex in the synthetic zeolites by complexation effect. Simultaneously, the mechanism of NH_4^+–N adsorption by the synthetic zeolites was the ion exchange between NH_4^+ and Na^+. The adsorption capacity developed with the increase of the NH_4^+–N and PO_4^{3-}–P concentration, and the maximum adsorption capacity depended on the properties of zeolites [32]. On the condition of the same amount addition of zeolites, a higher initial concentration of NH_4^+–N and PO_4^{3-}–P could provide more adsorption driving force [45], which could develop NH_4^+–N and PO_4^{3-}–P adsorption on the surface of the synthetic zeolites [46].

3.4. Recycle experiment of the synthetic zeolites

Insufficient zeolite recycle rate was the key obstacle for sustainable utilization [47]. In order to achieve cost saving and practical engineering application, the experiment was conducted to examine the reusability of the synthetic zeolites (Fig. 9). According to Eq. (4), the value of the adsorption capacity of PO_4^{3-}–P and NH_4^+–N by the recycled synthetic zeolites at equilibrium was 0.31 mg·g^{-1} and 0.55 mg·L^{-1}, respectively. Compared to the adsorption capacity of initial synthetic zeolites, the corresponding value of that was 0.35 mg·g^{-1} and 0.61 mg·L^{-1}, the equilibrium adsorption capacity of the recycled synthetic zeolites was equivalent to that of the initial synthetic zeolites. Therefore, it was suggested that the higher gradient of the solute could force adsorbates to diffuse deeply inside the zeolite channels with sufficient adsorbates, and the diffusion of PO_4^{3-}–P and NH_4^+–N could not be a restricted impact factor at the appropriate reaction time [32]. This process is mainly used for the chemical synthetic zeolites, the adsorption residence time was about 2 h, and 1.25 kg of synthetic zeolites were added into per ton of wastewater. The raw materials of synthetic zeolites were mainly used by kaolin (0.23 USD/kg, 1.2 kg), and NaOH (0.075 USD/kg, 0.16 kg), and the cost of adsorption process for per ton wastewater was only 0.28 USD. And according to the statistics, synthetic zeolites market will reach 2.7 bn of USD by 2028 with a compound annual growth rate of 3.5% [48]. Therefore, the synthetic zeolites have a great potential application in the future.

The good reusability and positive adsorption performance of the synthetic zeolites on PO_4^{3-}–P and NH_4^+–N removal in this study provided a potential strategy for the use of the synthetic zeolites in the management of nitrogen and phosphorus pollution. The advantage of this strategy existed that the synthetic zeolites was cost-effective because of the wide distribution of its raw materials in

nature. Meanwhile, challenges that should be considered carefully include how to apply the positive adsorption and the reusability property of the synthetic zeolites to practical engineering.

4. Conclusions

This study successfully proved the synthetic zeolites that produced by kaolin could simultaneously and effectively remove nitrogen and phosphorus from urban sewage. And the synthetic zeolites were used as a kind of mesoporous materials with large specific surface area and uneven pore-size distribution. Furthermore, ammonium nitrogen removal depends on cation exchange by zeolites, and the phosphorus removal depended on the ionic bond between PO_4^{3-} and the aluminum complex in the synthetic zeolites by complexation effect. Finally, the synthetic zeolites had a good reusability and positive adsorption performance. These results offer a new alternative for the sustainable use of zeolites and the removal of nitrogen and phosphorus from urban sewage by adsorption simultaneously. In future, the development of the eco-friendly synthetic zeolites is necessary to improve for practical engineering application.

Competing statements

We declare that we have no financial and personal relationships with other people or organizations that can inappropriately influence our work, there is no professional or other personal interest of any nature or kind in any product, service and/or company that could be construed as influencing the position presented in, or the review of, the manuscript entitled "Simultaneous removal of nitrogen and phosphorus from urban sewage by synthetic zeolites adsorption: performance, characterization, and mechanism".

Ethics approval and consent to participate

Not applicable

Consent for publication

Not applicable

Availability of data and materials

The authors confirm that the data supporting the findings of this study are available within the article.

Funding

This work was supported by the fund project of National Engineering Research Center of Bioenergy (Grant Nos. 2021B003), and the project of National Key Research and Development Program (Grant Nos. 2019YFC1803800-02).

Author contributions

All authors contributed to the study conception and design. [Rui Zhao]: Conceptualization, Investigation, Data analysis, Writing – review & editing. [Likun Huang]: Validation, Supervision, Writing – review & editing. [Guangzhi Wang]: Validation, Supervision, Funding acquisition, Writing – review & editing. [Hongfang Chen]: Conceptualization, Investigation, Data analysis, Writing – review & editing. [Simin Zhou]: Writing – review & editing. [Xiyu Sun]: Writing – review & editing. [Dongdong Wang]: Writing – review & editing. [Zhe Li]: Writing – review & editing. All authors commented on previous versions of the manuscript. All authors read and approved the final manuscript.

References

[1] E. Kirsten, M. Jiri, S. Karl, A review of water reuse and recycling, with reference to Canadian practice and potential: 1. Incentives and implementation, Water Qual. Res. J. Can., 39 (2004) 1–12.
[2] S.D.N. Freeman, O.J. Morin, Recent developments in membrane water reuse projects, Desalination, 103 (1995) 19–30.
[3] P. Jing, Z. Wang, Analysis of influencing factors of groundwater nitrate nitrogen driven by sewage reuse, IOP Conf. Ser.: Earth Environ. Sci., 766 (2021) 12–24.
[4] C.-W. Liu, Y. Sung, B.-C. Chen, H.-Y. Lai, Effects of nitrogen fertilizers on the growth and nitrate content of lettuce (*Lactuca sativa* L.), Int. J. Environ. Res. Public Health, 11 (2014) 4427–4440.
[5] T.L. Ng, W. Eheart, X. Cai, J.B. Braden, G.F. Czapar, Agronomic and stream nitrate load responses to incentives for bioenergy crop cultivation and reductions of carbon emissions and fertilizer use, J. Water Resour. Plann. Manage., 140 (2014) 112–120.
[6] K. Wu, Y. Li, T. Liu, N. Zhang, M. Wang, S. Yang, W. Wang, P. Jin, Evaluation of the adsorption of ammonium-nitrogen and phosphate on a granular composite adsorbent derived from zeolite, Environ. Sci. Pollut. Res., 26 (2019) 17632–17643.
[7] H. Li, Y. Li, J. Guo, Y. Song, Y. Hou, C. Lu, Y. Han, X. Shen, B. Liu, Effect of calcinated pyrite on simultaneous ammonia, nitrate and phosphorus removal in the BAF system and the Fe^{2+} regulatory mechanisms: electron transfer and biofilm properties, Environ. Res., 194 (2021) 110708, doi: 10.1016/j.envres.2021.110708.
[8] Y. Li, J. Guo, H. Li, Y. Song, Z. Chen, C. Lu, Y. Han, Y. Hou, Effect of dissolved oxygen on simultaneous removal of ammonia, nitrate and phosphorus via biological aerated filter with sulfur and pyrite as composite fillers, Bioresour. Technol., 296 (2020) 122340, doi: 10.1016/j.biortech.2019.122340.
[9] D.M. Mahapatra, G.S. Murthy, Long term evaluation of a pilot scale multimodal algal bioprocess for treatment of municipal wastewater, J. Cleaner Prod., 311 (2021) 127690, doi: 10.1016/j.jclepro.2021.127690.
[10] Y. Zhang, G.B. Douglas, L. Pu, Q. Zhao, Y. Tang, W. Xu, B. Luo, W. Hong, L. Cui, Z. Ye, Zero-valent iron-facilitated reduction of nitrate: chemical kinetics and reaction pathways, Sci. Total Environ., 598 (2017) 1140–1150, doi: 10.1016/j.scitotenv.2017.04.071
[11] L. El Hanache, B. Lebeau, H. Nouali, J. Toufaily, T. Hamieh, T. Jean Daou, Performance of surfactant-modified *BEA-type zeolite nanosponges for the removal of nitrate in contaminated water: effect of the external surface, J. Hazard. Mater., 364 (2019) 206–217.
[12] K.S. Haugen, M.J. Semmens, P.J. Novak, A novel in situ technology for the treatment of nitrate contaminated groundwater, Water Res., 36 (2002) 3497–3506.
[13] Y. Yurekli, Determination of adsorption characteristics of synthetic NaX nanoparticles, J. Hazard. Mater., 378 (2019) 120743, doi: 10.1016/j.jhazmat.2019.120743.
[14] C. Qin, R. Wang, W. Ma, Characteristics of calcium adsorption by Ca-selectivity zeolite in fixed-pH and in a range of pH, Chem. Eng. J., 156 (2010) 540–545.
[15] X. Liu, R. Wang, Effective removal of hydrogen sulfide using 4A molecular sieve zeolite synthesized from attapulgite, J. Hazard. Mater., 326 (2017) 157–164.

[16] M. Pérez-Page, J. Makel, K. Guan, S. Zhang, J. Tringe, R.H.R. Castro, P. Stroeve, Gas adsorption properties of ZSM-5 zeolites heated to extreme temperatures, Ceram. Int., 42 (2016) 15423–15431.
[17] R. Yan, S. Lin, Y. Li, W. Liu, Y. Mi, C. Tang, L. Wang, P. Wu, H. Peng, Novel shielding and synergy effects of Mn-Ce oxides confined in mesoporous zeolite for low temperature selective catalytic reduction of NO_x with enhanced SO_2/H_2O tolerance, J. Hazard. Mater., 396 (2020) 122592, doi: 10.1016/j.jhazmat.2020.122592.
[18] Y. Nomura, S. Fukahori, T. Fujiwara, Removal of sulfamonomethoxine and its transformation by-products from fresh aquaculture wastewater by a rotating advanced oxidation contactor equipped with zeolite/TiO_2 composite sheets, Process Saf. Environ. Prot., 134 (2020) 161–168.
[19] J. Wang, W. Jin, H. Guo, X. Wang, J. Liu, Experimental study on ammonia nitrogen adsorption performance of zeolite powder, Chem. Eng. Trans., 46 (2015) 79–84.
[20] L. Lin, Z. Lei, L. Wang, X. Liu, Y. Zhang, C. Wan, D.-J. Lee, J.H. Tay, Adsorption mechanisms of high-levels of ammonium onto natural and NaCl-modified zeolites, Sep. Purif. Technol., 103 (2013) 15–20.
[21] X. Guo, X. Cui, H. Li, B. Xiong, Purifying effect of biochar-zeolite constructed wetlands on arsenic-containing biogas slurry in large-scale pig farms, J. Cleaner Prod., 279 (2021) 123579, doi: 10.1016/j.jclepro.2020.123579.
[22] R.S. Bowman, Applications of surfactant-modified zeolites to environmental remediation, Microporous Mesoporous Mater., 61 (2003) 43–56.
[23] J.-I. Lee, J.-K. Kang, J.-S. Oh, S.-C. Yoo, C.-G. Lee, E.H. Jho, S.-J. Park, New insight to the use of oyster shell for removing phosphorus from aqueous solutions and fertilizing rice growth, J. Cleaner Prod., 328 (2021) 129536, doi: 10.1016/j.jclepro.2021.129536.
[24] C. Wang, D. Ren, G. Harle, Q. Qin, L. Guo, T. Zheng, X. Yin, J. Du, Y. Zhao, Ammonia removal in selective catalytic oxidation: influence of catalyst structure on the nitrogen selectivity, J. Hazard. Mater., 416 (2021) 125782, doi: 10.1016/j.jhazmat.2021.125782.
[25] D. Wang, Z. Qi, Z. Xing, F. Lei, Control of chloride ion corrosion by $MgAlO_x$/$MgAlFeO_x$ in the process of chloride deicing, Environ. Sci. Pollut. Res. Int., 29 (2022) 9269–9281.
[26] APHA Association, Standard Methods for the Examination of Water and Wastewater, American Public Health Association (APHA), USA, 2005.
[27] I. Langmuir, The adsorption of gases on plane surfaces of glass, mica and platinum, J. Am. Chem. Soc., 40 (1918) 1361–1403.
[28] P. He, Y. Zhang, X. Zhang, H. Chen, Diverse zeolites derived from a circulating fluidized bed fly ash based geopolymer for the adsorption of lead ions from wastewater, J. Cleaner Prod., 312 (2021) 127769, doi: 10.1016/j.jclepro.2021.127769.
[29] G. Blanchard, M. Maunaye, G. Martin, Removal of heavy metals from waters by means of natural zeolites, Water Res., 18 (1984) 1501–1507.
[30] H. Hazar, R. Tekdogan, H. Sevinc, Determination of the effects of oxygen-enriched air with the help of zeolites on the exhaust emission and performance of a diesel engine, Energy, 236 (2021) 121455, doi: 10.1016/j.energy.2021.121455.
[31] C. Wan, S. Ding, C. Zhang, X. Tan, W. Zou, X. Liu, X. Yang, Simultaneous recovery of nitrogen and phosphorus from sludge fermentation liquid by zeolite adsorption: mechanism and application, Sep. Purif. Technol., 180 (2017) 1–12.
[32] Z. Razavi, N. Mirghaffari, A. Akbar Alemrajabi, F. Davar, M. Soleimani, Adsorption and photocatalytic removal of SO_2 using natural and synthetic zeolites-supported TiO_2 in a solar parabolic trough collector, J. Cleaner Prod., 310 (2021) 127376, doi: 10.1016/j.jclepro.2021.127376.
[33] F. Espejel Ayala, Y. Reyes-Vidal, J. Bacame-Valenzuela, J. Pérez-García, A. Hernández Palomares, Natural and Synthetic Zeolites for the Removal of Heavy Metals and Metalloids Generated in the Mining Industry, M.P. Shah, S.R. Couto, V. Kumar, Eds., New Trends in Removal of Heavy Metals from Industrial Wastewater, Elsevier, Amsterdam, 2021, pp. 631–648.
[34] J. Szerement, A. Szatanik-Kloc, R. Jarosz, T. Bajda, M. Mierzwa-Hersztek, Contemporary applications of natural and synthetic zeolites from fly ash in agriculture and environmental protection, J. Cleaner Prod., 311 (2021) 127461, doi: 10.1016/j.jclepro.2021.127461.
[35] M.M. Mohamed, W.A. Bayoumy, M. Khairy, M.A. Mousa, Synthesis of micro–mesoporous TiO_2 materials assembled via cationic surfactants: morphology, thermal stability and surface acidity characteristics, Microporous Mesoporous Mater., 103 (2007) 174–183.
[36] C. Zhang, B. Zhou, Z. Li, Study on simultaneous degradation of nitrogen and phosphorus in wastewater from sludge dewatering removal by mixing sodium and lanthanum modified zeolite, IOP Conf. Ser.: Earth Environ. Sci., 601 (2020) 012019, doi: 10.1088/1755-1315/601/1/012019.
[37] H. Zhu, L. Li, W. Chen, Y. Tong, X. Wang, Controllable synthesis of coral-like hierarchical porous magnesium hydroxide with various surface area and pore volume for lead and cadmium ion adsorption, J. Hazard. Mater., 416 (2021) 125922, doi: 10.1016/j.jhazmat.2021.125922.
[38] N. Widiastuti, H. Wu, H.M. Ang, D. Zhang, Removal of ammonium from greywater using natural zeolite, Desalination, 277 (2011) 15–23.
[39] N. Merilaita, T. Vastamäki, A. Ismailov, E. Levänen, M. Järveläinen, Stereolithography as a manufacturing method for a hierarchically porous ZSM-5 zeolite structure with adsorption capabilities, Ceram. Int., 47 (2021) 10742–10748.
[40] L. Xu, T. Jiang, P. Yu, Q. Zhao, Experimental study on the effect of combined modified aluminum and magnesium and phosphorus removal of zeolite, Bulg. Chem. Commun., 48 (2016) 80–83.
[41] G.L.D. Rivera, A.M. Hernández, A.F.P. Cabello, E.L.R. Barragán, A.L. Montes, G.A.F. Escamilla, L.S. Rangel, S.I.S. Vazquez, D.A. De Haro Del Río, Removal of chromate anions and immobilization using surfactant-modified zeolites, J. Water Process Eng., 39 (2021) 101717, doi: 10.1016/j.jwpe.2020.101717.
[42] D.R. Durham, L.C. Marshall, J.G. Miller, A.B. Chmurny, New composite biocarriers engineered to contain adsorptive and ion-exchange properties improve immobilized-cell bioreactor process dependability, Appl. Environ. Microbiol., 60 (1994) 4178–4181.
[43] Y. Watanabe, H. Yamada, H. Kokusen, J. Tanaka, Y. Moriyoshi, Y. Komatsu, Ion exchange behavior of natural zeolites in distilled water, hydrochloric acid, and ammonium chloride solution, Sep. Sci. Technol., 38 (2007) 1519–1532.
[44] J. Wen, H. Dong, G. Zeng, Application of zeolite in removing salinity/sodicity from wastewater: a review of mechanisms, challenges and opportunities, J. Cleaner Prod., 197 (2018) 1435–1446.
[45] A. Demir, A. Günay, E. Debik, Ammonium removal from aqueous solution by ion-exchange using packed bed natural zeolite, Water SA, 28 (2002) 329–336.
[46] Q. Du, S. Liu, Z. Cao, Y. Wang, Ammonia removal from aqueous solution using natural Chinese clinoptilolite, Sep. Purif. Technol., 44 (2005) 229–234.
[47] J. Chen, X. Wang, S. Zhou, Z. Chen, Effect of alkalinity on bio-zeolite regeneration in treating cold low-strength ammonium wastewater via adsorption and enhanced regeneration, Environ. Sci. Pollut. Res., 26 (2019) 28040–28051.
[48] F. Group, Synthetic Zeolites Market Will Reach $2.7 bn by 2028 with a CAGR of 3.5%, Focus on Catalysts, 2022.